AD-A129 300 INVESTIGATION OF LITHIUM THIONYL CHLORIDE BATTERY SAFETY HAZARDS(U) GTE COMMUNICATIONS PRODUCTS CORP WALTHAM MA POWER SYSTEMS OPERATION R C MCDONALD 1/1

UNCLASSIFIED 31 MAR 82 N60921-81-C-0229 F/G 10/2 NL

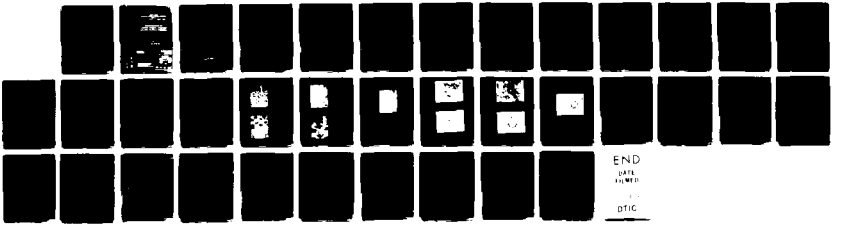

END

DATE FILMED

DTIC

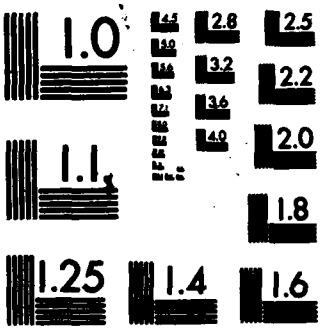

MICROCOPY RESOLUTION TEST CHART
NATIONAL BUREAU OF STANDARDS-1963-A

CDRL A002
Quarterly Technical Progress Report
Period
1 January 1982 — 31 March 1982

INVESTIGATION OF LITHIUM THIONYL CHLORIDE BATTERY SAFETY HAZARDS

Prepared under:

Contract N60921-81-C-0229
for
Naval Surface Weapons Center
Silver Spring, Maryland 20910

Robert C. McDonald
Principal Investigator

GTE Products Corporation
Strategic Systems Division
Power Systems Operation
520 Winter Street
Waltham, Massachusetts 02254

TABLE OF CONTENTS

LIST OF FIGURES

ABSTRACT

Scanning electron and optical microscopic investigation of an overdischarged cathode from a cathode limited Li/$SOCl_2$ cell reveal a three-dimensional reticulated lithium dendrite structure. Individual dendrites do not grow any longer than about 50 microns or any thicker than about 4 microns in diameter before branching at random angles.

E.S.R. spectra of 50% and 100% overdischarged anode limited cells reveal a third chemical species carrying an unpaired electron which is distinct from the two radical species observed during discharge.

No significant difference is observed between the Raman spectra of 100% discharged electrolyte and 50% cathode limited overdischarged electrolyte. The same holds true for infrared spectra.

The Raman spectrum of 90% anode limited overdischarged electrolyte shows most of the peaks occuring at 100% discharge in addition to 687, 727, 819, and 854 cm^{-1}. The infrared spectrum of the same solution shows most of the features occuring at 100% discharge in addition to the reduction of 981 cm^{-1} and growth of peaks at 1397, 1085, 1070 (shoulder) 661 and 602 cm^{-1}. Peaks at 1070 and 661 always occur weakly in discharged electrolyte spectra and are quite strong in the spectrum of Li_2SO_4 saturated electrolyte

A. Raman Emission Spectroscopy

The accompanying table lists the Raman emission observed in electrolyte from the anode limited overdischarged cell (90%) compared with electrolyte from the cathode limited overdischarged (30%) cell for comparison. Not surprisingly, the anode limited spectra is richer in emissions. All emissions from cathode limited overdischarge have counterparts in anode limited overdischarge with the exception of weak bands at 280 and 332 cm^{-1}. Both of these are also observed in 100% discharged electrolyte (QRI).

Raman Emission for Overdischarged Electrolyte

Anode Limited Overdischarge (90%)	Cathode Limited Overdischarge (30%)
96 S	
145 asym	
210 M	210 M
244 vw	
	280 w sharp
304 w	305 w
	332 vw
355 s	358 m
461 vw, sh.	
480 vw, sh	475 w
491 vw, sh	
510 m, br.	509 m
687 w	
727 w	
819 vw	
854 vw	
1162 w	1159 w
1231 w	1229 vw

S=Strong, W=Weak, M=Medium, Sh=Shoulder, br=broad

Emissions at 96 and 145 cm^{-1} are low enough to be due to lattice mode vibration of suspended solids yet this sample was the clearest of any of the electrolyte samples examined.

QRI = First Quarterly Report

Most emissions in the 200-500 cm^{-1} range appear to be associated with SO_2, $SOCl_2$, and their solute-solvent complexes with $LiAlCl_4$.

Chlorine gas is expected to emit near 565 cm^{-1} (33). The closest observed line at 510 occurs both in anode and cathode limited cells and it is doubtful that chlorine can form on the anode with lithium still present. Thus, there is no evidence for Cl_2 from the Raman spectra.

Raman peaks in the 600-900 cm^{-1} may be associated with chlorine oxides formed in the absence of lithium as suggested by Salmon et al (3). Chi and Andrews (30) have reported Raman spectra for Cl_2O, Cl-ClO, ClO, and Cl=O-Cl=O isomers formed by mercury arc photolysis in an argon matrix. These are summarized below:

Cl_2O	638, 298, 678 cm^{-1} all intense
C-ClO	962, 378, 241 cm^{-1} all intense
ClO	850 cm^{-1} weak
Cl=O-Cl=O	995, 986 cm^{-1} intense doublet

Thus, there is some evidence for Cl_2O and ClO in the Raman and infrared (vida infra) of anode limited overdischarged electrolyte though it is difficult to imagine how such high oxidation states of chlorine can be produced at a nickel substrate polarized to less than the observed 0.1 volts anodic to lithium.

B. Infrared Spectroscopy

Infrared spectra are given in the appendix for cathode limited 30% overdischarge, anode limited 90% overdischarged and Li_2SO_4 saturated electrolyte. The last spectrum was prepared under a different project and is included because of its marked similarity to anode limited overdischarged electrolyte.

The peaks at 1070 cm^{-1} and 661 cm^{-1} appear already in 100% discharged electrolyte from anode limited cells (QRI). They develop more fully in Li_2SO_4 saturated electrolyte cathode limited overdischarged electrolyte and as a shoulder on 1085 cm^{-1} in anode limited overdischarged electrolyte. Solman et al (11) have suggested that SO^{2+} resulting from oxidation in overdischarging anode limited cells absorbs at 1070 cm^{-1}, while a peak at 640 cm^{-1} in the same electrolyte was ascribed to Cl_2O. Our studies do not show any distinct peak at 690 cm^{-1} but we do observe a peak at 661 cm^{-1} under a variey of conditions.

Full interpretation of these and the Raman spectra await further control experiments and in situ studies.

C. Electron Spin Resonance Spectroscopy

The two ESR resonance peaks observed on discharge, I with g= 1.9990($\pm$5) and II with g= 1.9864($\pm$1) are still observed on overdischarge though they do not grow significantly. Both peaks can be seen on Spectrum ESR-2 when both solid and liquid are present in electrolyte from a cathode limited overdischarged cell. When the solids are moved out of the ESR cavity (ESR-1) peak II disappears. When the instrument gain is increased Spectrum ESR-2 reveals a hyperfine splitting pattern (ESR-3) centered around peak II.

All earlier spectra reported were recorded on samples containing both liquid and solid. Thus peak II appears to be a solid free radical or perhaps Species I complexed to solid in such a way as to shift the electron spin density and resulting in a distinct g factor.

It is interesting to note that the electrolyte from the anode limited 100% overdischarged cell was quite clear with no solids settling out. Thus only peak I is observed (ESR-4).

The principle difference between anode and cathode limited cells appears to be that species II associated with solids in discharged and cathode limited overdischarged cells is consumed during overdischarge of anode limited cells.

The third ESR peak mentioned in the First Quarterly Report is seen as a shoulder on peak I (Peak III) on overdischarge of cathode limited cells. It disappears after 2 weeks leaving peak I as a slightly assymetric peak.

In summary, the ESR spectra of cathode limited overdischarge electrolyte is characterized by the formation of transient Species III and hyperfine splitting of Species II. The ESR spectrum of both anode and cathode limited overdischarged electrolyte contains Species I apparently a residue of cell discharge.

D. Morphological Studies

The cell used to investigate dendrite morphology in cathode limited cells during overdischarge consisted of a single 3.0 x 3.5 cm Teflon bonded carbon cathode 0.96 mm thick positioned between two 3.0 x 3.5 cm Li anodes. The cathode and two lithium anodes were parallel and separated 6 mm. The Li electrodes were fabricated by pressing two 0.76 mm sheets of Li foil on both sides of a 5 Ni 10 - 2/10 Exmet grid to which was welded a 0.76 mm dia Ni lead wire. The cathode lead was attached by scraping away a 0.5 x 3.0 cm section of the carbon at the top of the electrode (cf. Figure 1). Since the electrodes were held rigidly in place with the thick Ni lead wires no separator was required thus allowing an unobstructed view of all electrode surfaces. The cell was evacuated to 200 Hg then filled with 1.8M $LiAlCl_4/SOCl_2$ electrolyte.

Discharge and overdischarge were carried out galvanostically at a total cell current of 90 mA which corresponds to 5 mA/cm^2 on the surface of the cathode. As soon as overdischarge was terminat electrolyte was drained out of the cell and the cell was evacuated for 15 minutes. Finally the cell was disassembled in the dry room and the carbon cathode placed in a vacuum desiccator for several hours to remove all $SOCl_2$ to permit SEM photographs to be taken.

The optical microphotographs were taken with a Bausch & Lomb Stereo Zoon 7 microscope equipped with a 3-1/4 x 4-1/4 in Polaroid camera. The scanning electron microscope (SEM) studies were carried out with a JEOL Model V3.

The cell delivered 48.3 $mAhr/cm^2$ to 0.50V and 58.5 $mAhr/cm^2$ to 0.00V at 5 mA/cm^2 constant current. On overdischarge at 5 mA/cm^2 the polarity of the cell reversed so that the cathode reached a maximum potential of -210 mV versus the Li anode. After 2.4 hours of overdischarge (24 $mAhr/cm^2$) the current was stopped to avoid a short current because the Li dendrites on the cathode almost reached the Li anode. Thus it was only possible to overdischarge the cell 41%. During overdischarge the cell potential rose from -? . mV to -120 mV most likely because the growth of dendri- on the carbon surface gradually increased

the area of Li substrate available for Li deposition and decreased the distance between the growing dendrites and the Li electrode.

Figures 1 to 10 show various aspects of a single carbon electrode viewed face on and in cross section under an optical microscope (Figures 1 - 5) and with a scanning electron microscope (SEM) (Figures 6 - 10). Figure 1 gives an overall view of the top of the electrode at 5X magnification which is helpful in locating the position of later microphotographs at higher magnification. The Ni lead which was mostly covered with dendrites but smooth near the top can be seen in the upper part of Figure 1. The upper part of the Ni lead was free from dendrites because it was above the surface of the electrolyte. The contrast between the parts on the Ni lead which are smooth and those covered with Li deposits give a clear indication of the thickness of the deposits.

Figure 2 shows the area in the center of Figure 1 at twice the magnification (i.e. 10X vs. 5X magnification). Figure 3 shows the Li dendrite deposits on the surface of the carbon electrode at 30X magnification at a point slightly below center in Figure 2 and slightly at the left. Figure shows the Li dendrite encrusted lead as it meets the Exmet grid at 10 X magnification compared to only 5X in Figure 1. Figure 6 shows a cross section of the 1 mm thick cathode at a magnification of 50 X. Lithium dendrites on the surface of the cathode are clearly visible but no Li deposits were observed in the interior of the cathode when many samples were examined. The large bright particles seen at the top of Figure 5 and the smaller particles seen in the interior were introduced when the cathode cross-section was cut.

Figure 6 is an SEM photograph of a cross section of the overdischarged cathode at a magnification of 160X seen at an angle of approximately 30°. The Li deposits on the surface of

the electrode are seen as well as two Li particles loosely attached to the interior cross section which again appear to be fragments from when the cross section was cut. A close examination of the clean cut carbon surface of the cross section shown in Figure 6 as well as several other places along the cross section revealed no signs of Li deposition inside the carbon as would be expected because electrostatic theory predicts the absence of a potential field in any cavity inside an electronic conductor. Electrochemical reaction occur in the interior of porous electrodes during discharge because ionic mobility occurs mainly by diffusion but during electrolysis caused by overdischarge or charge ionic mobility occurs mainly through electromigration which is dependent on the electric field.

Figure 7 shows an SEM photograph of the Li dendrites on the surface of the overdischarged carbon electrode as seen at 50X magnification. The SEM photograph as expected is similar to the optical photograph of the cathode as shown in Figure 3 but shows somewhat more detail since the magnification was increased from 30X to 50X. Figure 8 shows a small portion from the center of Figure 7 with the magnification increased to 300X. Third in this series, Figure 9 shows a small portion from the center of Figure 8 with the magnification increased from 300X to 1000X. The coiled spaghetti-like structure of the Li filaments which make up the Li nodules on the surface of the carbon electrode is a remarkable structural feature of considerabl practical importance. For example, since the nodules are porous and not solid, it is likely that they would not cause a serious short circuit problem in overdischarged cells. Furthermore the small diameter of the Li filaments (i.e. 4 microns), suggests that the filaments could easily grow through a glass fiber separator but could not carry significant currents should a short circuit occur when the dendrite grew to touch the Li electrode.

Schlaikjer et al have shown (32) that the LiCl passive film varies from 0.08 microns to 0.14 microns in thickness so one is forced to conclude that filaments have at least some lithium at

their core. Whether or not this metallic core runs continuously throughout the filament network back to the carbon cathode cannot be determined at this time.

Figure 10 shows a SEM photograph of Li dendrites growing on the Ni lead wire at 1000 x magnification. The Li dendrite structure on the Ni lead appears to be almost entirely of filaments without the plates or crystals seen in the nodules grown on the carbon surface. It is thought that the dendrites grown on Ni are almost entirely filaments because nucleation of Li dendrites occurs more easily on Ni than carbon with fewer better formed dendrites.

When interpreting the microphotographs of Li dendrites it should be kept in mind that in solution of the Li filaments are supported by the electrolyte and the dendrites are somewhat less compacted than in the photographs. Thus they are much more porous and less able to support even small short circuit currents than the microphotographs would tend to suggest.

The high surface area of the Li dendrites is of some concern since it could be the basis of a rapid reaction between the Li dendrites and discharge products such as elemental sulfur.

The Ostwald ripening studies are currently underway. A cell was discharged for 93.6 hours at 3.0 mA/cm^2 then overdischarged for about 8 hours. Photographs were taken of the dendrites through the glass window in the cell immediately at the end of overdischarge and after 15, 21 min, 4, 16.2 and 42 hrs. Preliminary results show that the Li dendrites lose a small amount of Li during the first 42 hours of storage. There is no evidence for dendrite growth at high points in the nodules on storage.

Lastly, needle crystals were observed in some areas of the cathode where electrolyte salts crystallized out on evacuation. Crystals of LiCl on the other hand form very rapidly so they are quite small and thus appear amophous at the magnifications used so far. Therefore, the LiCl coated lithium can be distinquished from the dried salts.

Electron Spin Resonance Spectra

1. Cathode limited 50% overdischarged electrolyte with liquid only.

2. Cathode limited 50% overdischarged electrolyte with liquids and solids.

3. Cathode limited 50% overdischarged electrolyte with liquids and solids. Increased gain.

4. Anode limited 100% overdischarged electrolyte with liquid only.

Fourier Transform Infrared Spectra

1. Fresh cathode limited 50% overdischarged electrolyte.

2. Two-day old anode limited 100% overdischarged electrolyte.

3. Li_2SO_4 saturated electrolyte.

REFERENCES

1. K. M. Abraham, R. M.Mank and G. L. Holleck, ERADCOM, DELET-TR-0564F Final Report for Contract No. DAABOF-78-C-0564m "Investigations of the Safety of $Li/SOCl_2$ Batteries".

2. K. M. Abraham and R. M. Mank, J. Electrochem. Soc. 127, 2091 (1980). "Some Chemistry in the $Li/SOCl_2$ cell".

3. D. J. Salmon, M. E. Adamczyk, L. L. Studer, L. L. Abels and J. C. Hall, Abstract No. 62, Electrochemical Society Meeting, 1980, Hollywood, Fla., "Spectroscopic Studies of the Hazards of $Li/SOCl_2$ Batteries During Cell Reversal.

4. W. P. Kilroy and S. D. James, J. Electrochemical Soc. 128, 93A (1981). "Promotion by Carbon of the Reactivity of Lithium with $SOCl_2$ and SO_2 - Effect on Lithium Battery Safety".

5. TRW Document, Qualification and Characterization Testing of Minuteman Lithium Power Source" (BMO Transmittal Serial No. 3054-KH-Kh 8900-WPF).

6. Final Report - Wyle Tests - System Demonstration MESP Contract No.

7. C. Schlaikjer, F. Goebel and N. Marincic, J. Electrochemical Soc., 126, 513, (1979).

8. Report No. 0001-141A2-3D, "Lithium Power Source Draft Final Engineering Report", Contract No. F04704-78-C-0001, March 1980. BMO, Page AJ-1 Appendix AJ.

9. Report No. AF WAL-TR-80-2121, F. Goebel, R. McDonald, and G. Younger, "Lithium Inorganic Electrolyte Battery", Contract No. 0001 Wright Patterson Air Force Base, p. 55.

10. F. Goebel, R. McDonald, and N. Marincic, Proc. of the 15th I.E.C.E.C. Meeting, Seattle, Wash., August 1980, "Performance Characteristics of the Minuteman Lithium Power Source".

11. D. J. Salmon, M. E. Adamczyk, L. L. Hendricks, L. L. Abels and J. C. Hall, Proceedings fo the Symposium on Lithium Batteries, H. J. VanKatasetty, 81-4, p. 65 (1981). "Spectroscopic Studies of the Hazards of $Li/SOCl_2$ Batteries During Anode Limited Cell Reversal".

12. "Raman Spectroscopy, Theory and Practice", Vols. 1, 2, Edited by H. A. Szymanski, Plenum Press, New York, 1970.

13. W. Ostwald, Z. Physik. Chem. Leipzig, 34, 495 (1900).

14. L. Harbury, J. Phys. Colloid Chem., 51, 382 (1947).

15. G. L. Holleck, M. J. Turchan and D. E. Toland, U. S. Army Econ, Fifth Quarterly Report, ECOM-74-0030-5 (April 1975).

16. J. Butler; Final Report No. AFCRL-70-0605, Contract F19628-68-C-056 (Sept. 30, 1970).

17. D. A. Skoog and J. K. Bartlett, Anal. Chem. 27 (3), 369 (1955).

18. K. French, P. Cukor, C. Persiani, J. Auborn, J. Electrochem. Soc. 121, 1045, (1974).

19. N. Marincic, F. Goebel, J. Appl. Electrochem. 8, 11, (1978).

20. A. N. Dey, Thin Solid Films 43, 131, (1977).

21. C. R. Schlaikjer, J. Electrochem. Soc. 126, 2168, (1979).

22. C. R. Schlaikjer, C. A. Young, M. Dobrusin, Report DELET-TR-78-0558.1F (May 1980).

23. K. M. Abraham, R. M. Mank and G. L. Holleck, Proceedings of the Symposium on Ambient Temperature Lithium Batteires, B. Owens and W. Margaliteds, 1979).

24. J. O. Besenhard, Carbon, 14, 111 (1976)

25. K. M. Abraham, G. L. Holleck and S. B. Brummer, Proc. of the Symp. on Battery Design and Optimization, S. Grass ed., The Electrochemical Society, N.J.,(1979).

26. K. M. Abraham, R. M. Monk and G. L. Holleck, EIC Corp., 2nd Quarterly Report, ERADCOM-DELET-TR-78-0564-2, July 1979.

27. D. A. Long and R. T. Bailey, Trans. Farad. Soc., 59, 594 (1963).

28. H. J. Bernstein and J. Powling, J. Chem. Phys., 18, 1018 (1950).

29. P. W. Schenk and R. Stendel, Angew. Chem. Internat. Edit 4, 402 (1965).

30. F. K. Chi and L. Andrews, J. Phys. Chem., 77, 3062 (1973).

31. R. Vogel-Hogler, Acta Phys. Austriaca, 1, 323 (1948).

32. C. Schlaikjer, C. A.Young and M. Dobrusin, ECOM Report No. DELET-TR-78-0558.1F, May 1970.

33. G. Hertzberg, Molecular Spectra Molecular Structure, Van Nostrand, Princeton (1950) O^{18} exchange for $SOCl_2$ in SO_2.

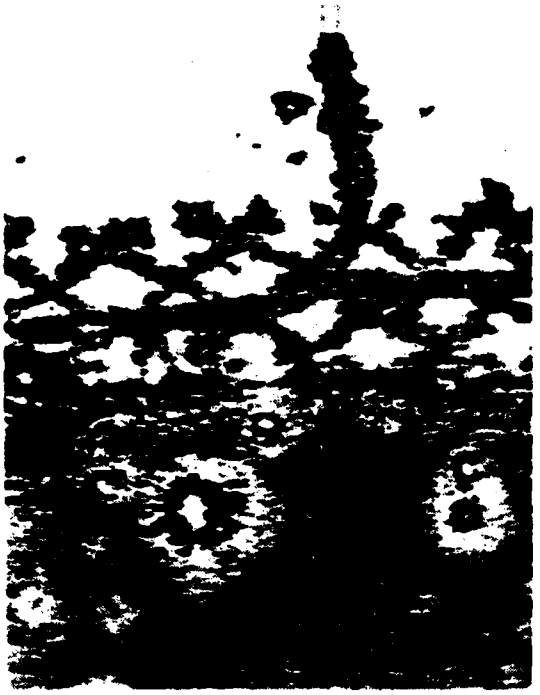

Figure 1.

Lithium Dendrites on Carbon Cathode and the Exposed Exmet Grid and Lead (5X Magnification)

Figure 2.

Lithium Dendrites on Carbon Cathode and Exposed Exmet Grid Directly Below the Lead (10X Magnification)

Figure 3

Lithium Dendrites on Carbon Cathode Surface
(30X Magnification)

Figure 4

Lithium Dendrites on Lead and Exmet Grid Above Cathode
(10X Magnification)

Figure 5

Optical Microphotograph of Cathode Cross Section
(50X Magnification)

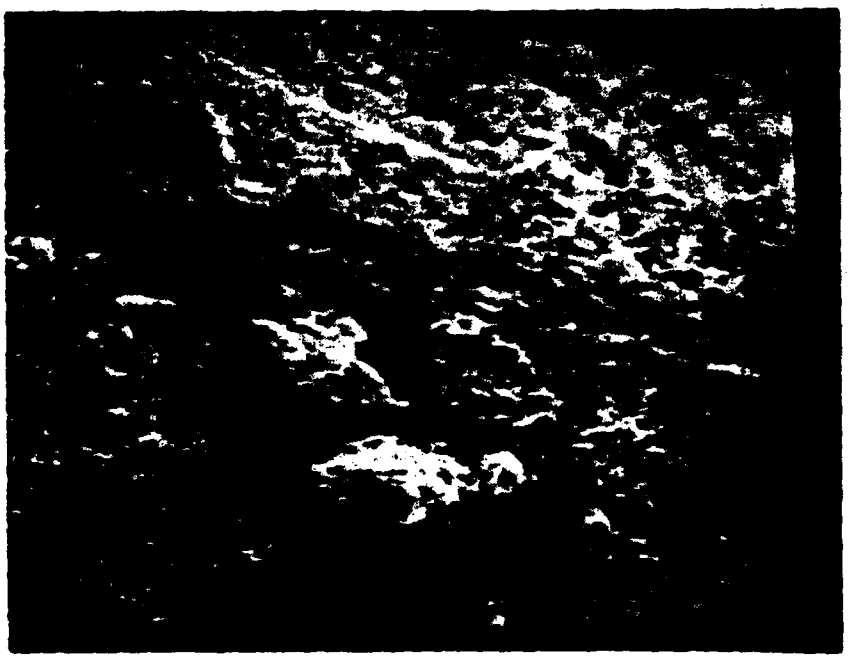

Figure 6

Scanning Electron Microscope Photograph of Cathode Cross Section (160X Magnification)

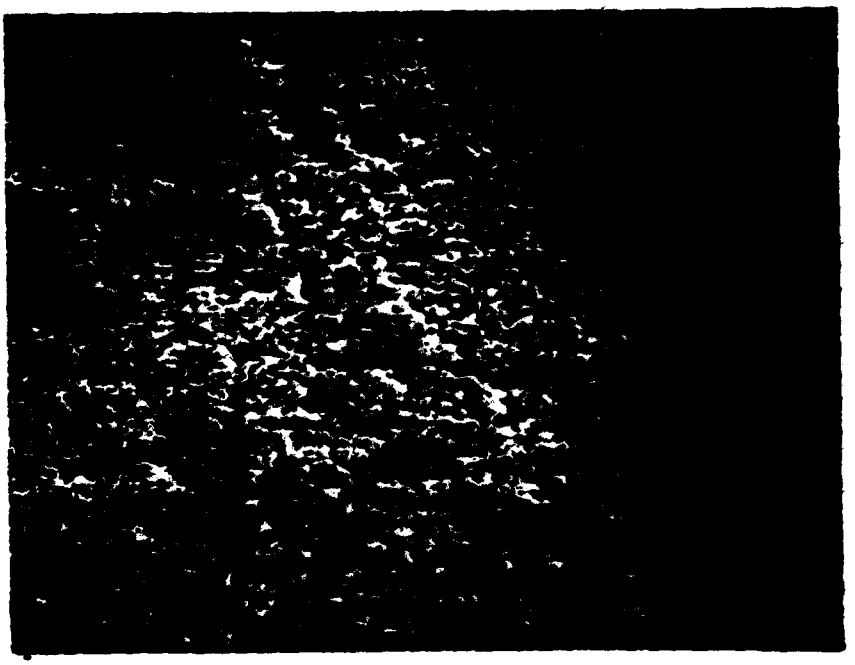

Figure 7

Scanning Electron Microscope Photograph of Lithium Dendrites on Carbon Cathode Surface (50X Magnification)

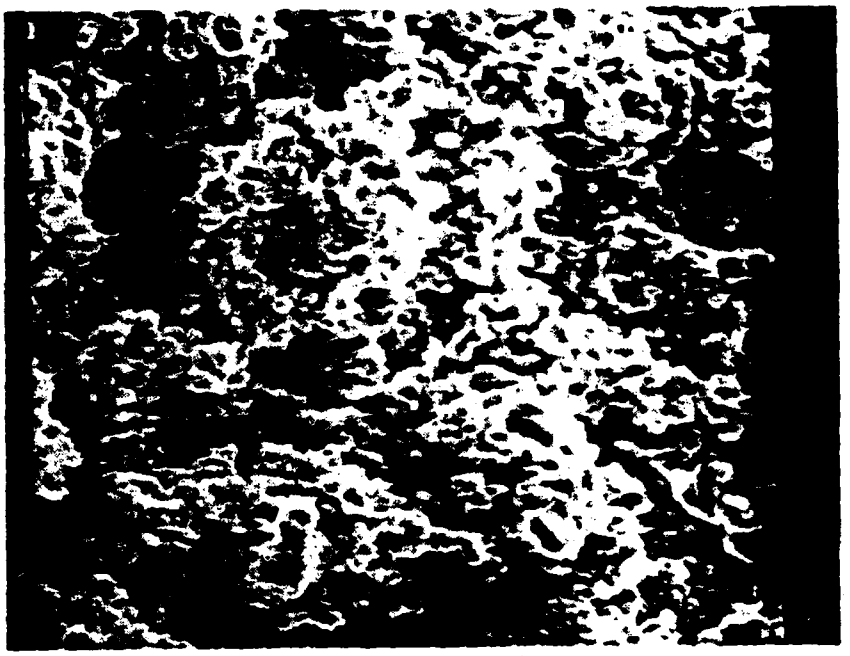

Figure 8

Scanning Electron Microscope Photograph of Lithium Dendrites on Carbon Cathode Surface (300X Magnification)

Figure 9

Scanning Electron Microscope Photograph of Lithium Dendrites on Carbon Cathode Surface (1000X Magnification)

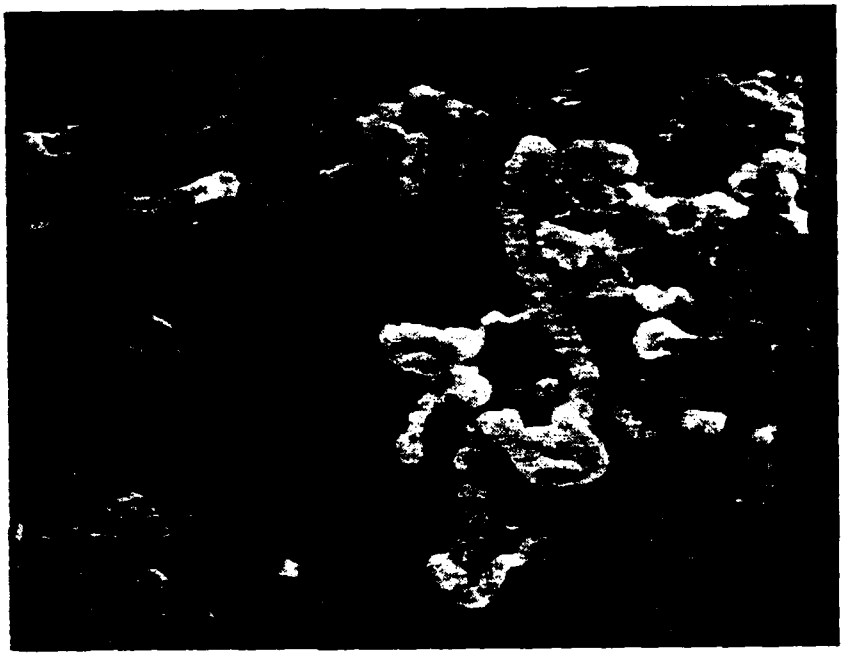

Figure 10

Scanning Electron Microscope Photograph of
Lithium Dendrites on Nickel Lead Wire
(1000X Magnification)

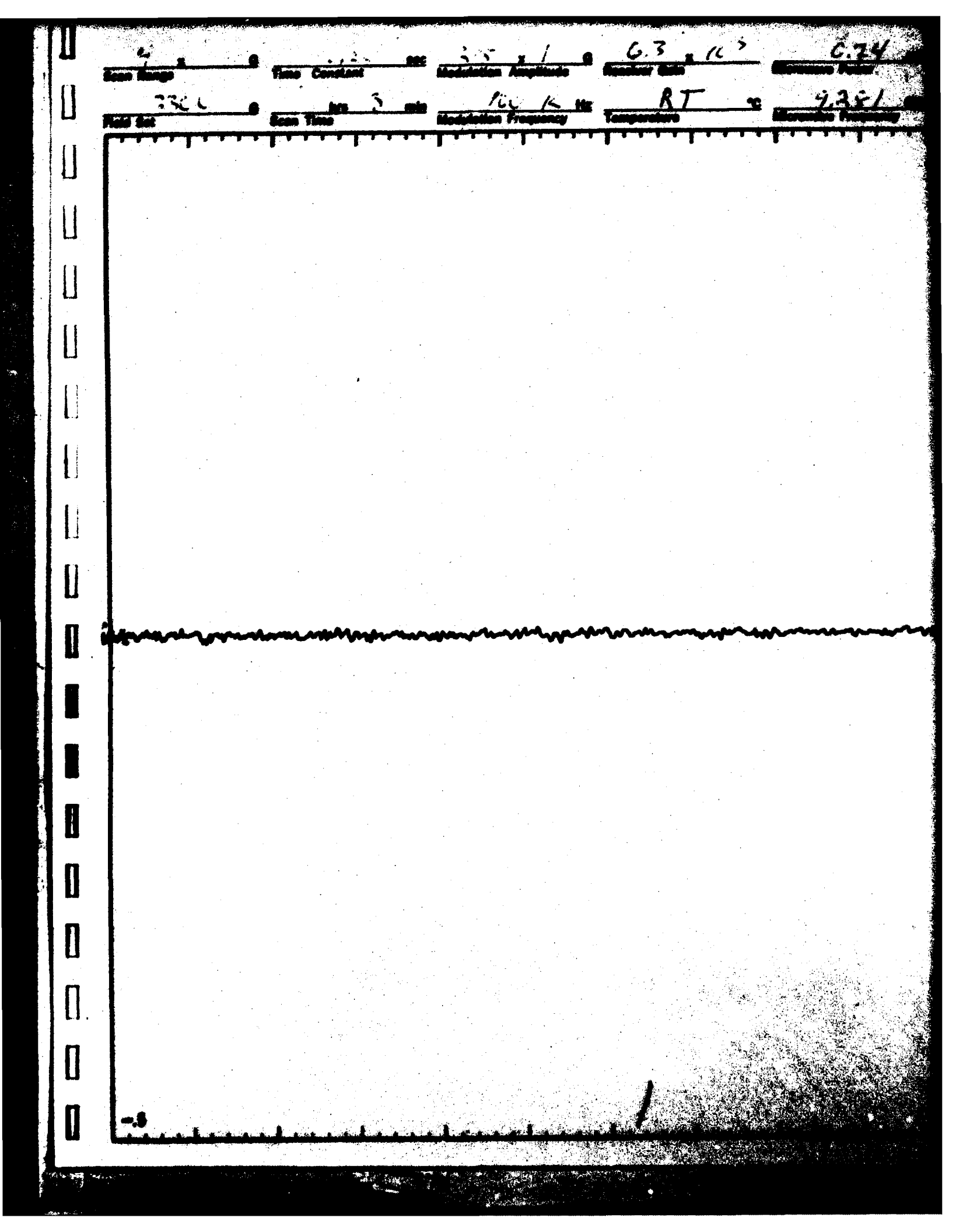
Scan Range
Time Constant
Modulation Amplitude
Modulation Frequency
Temperature
Scan Time
min
RT
-1

mW J Bennett
Operator

GHz 11/8 2 Ni solids presented to microwave cavity
Frequency Date Remarks

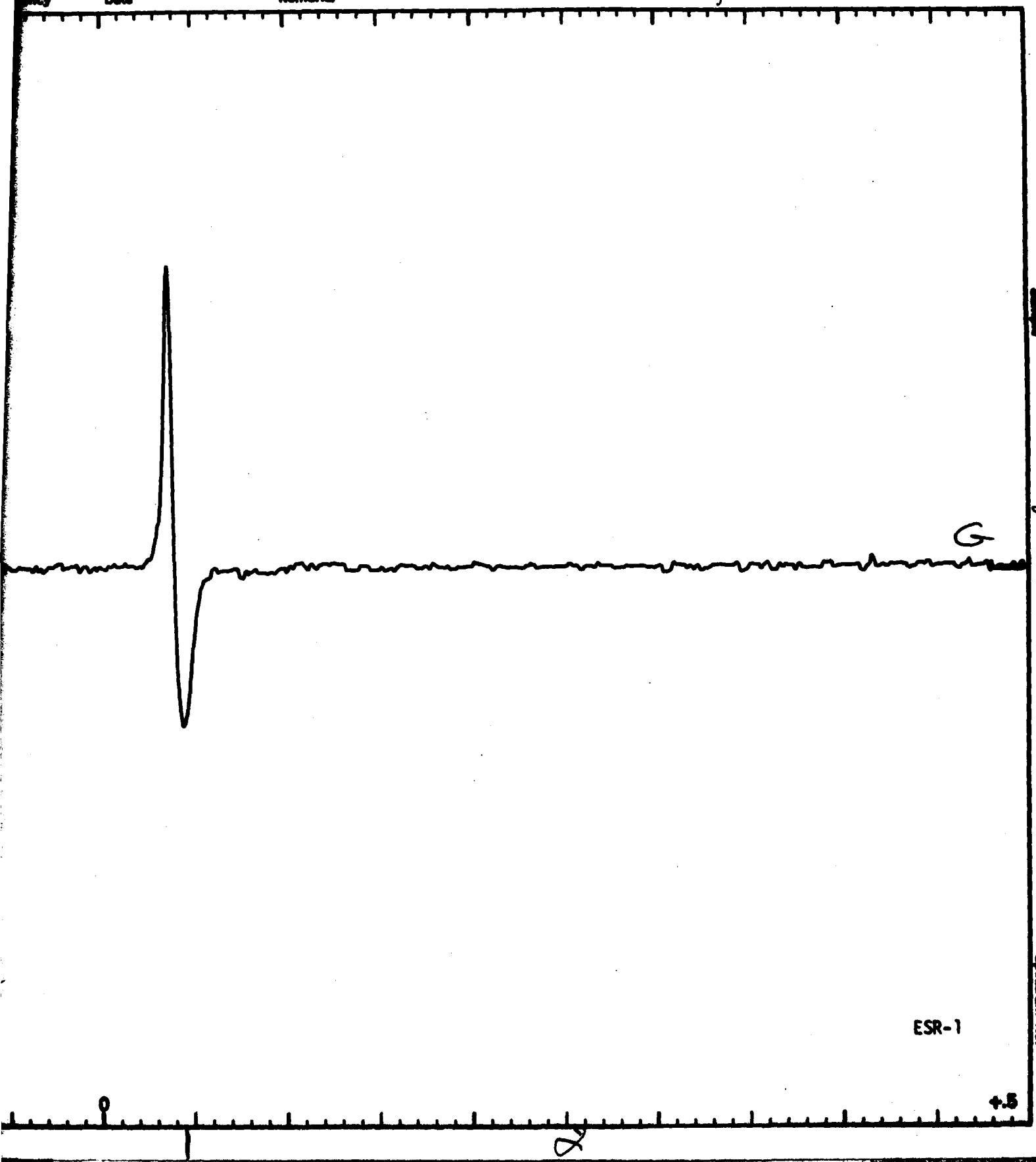

Scan Range 4 x 50 G | Time Constant .25 sec | Modulation Amplitude 2.5 x 1 G | Receiver Gain 6.3 x 10 | Microwave Power 10 mW

Field Set 3300 G | Scan Time hrs 8 min | Modulation Frequency 100 KHz | Temperature RT °C | Microwave Frequency 9281 MHz

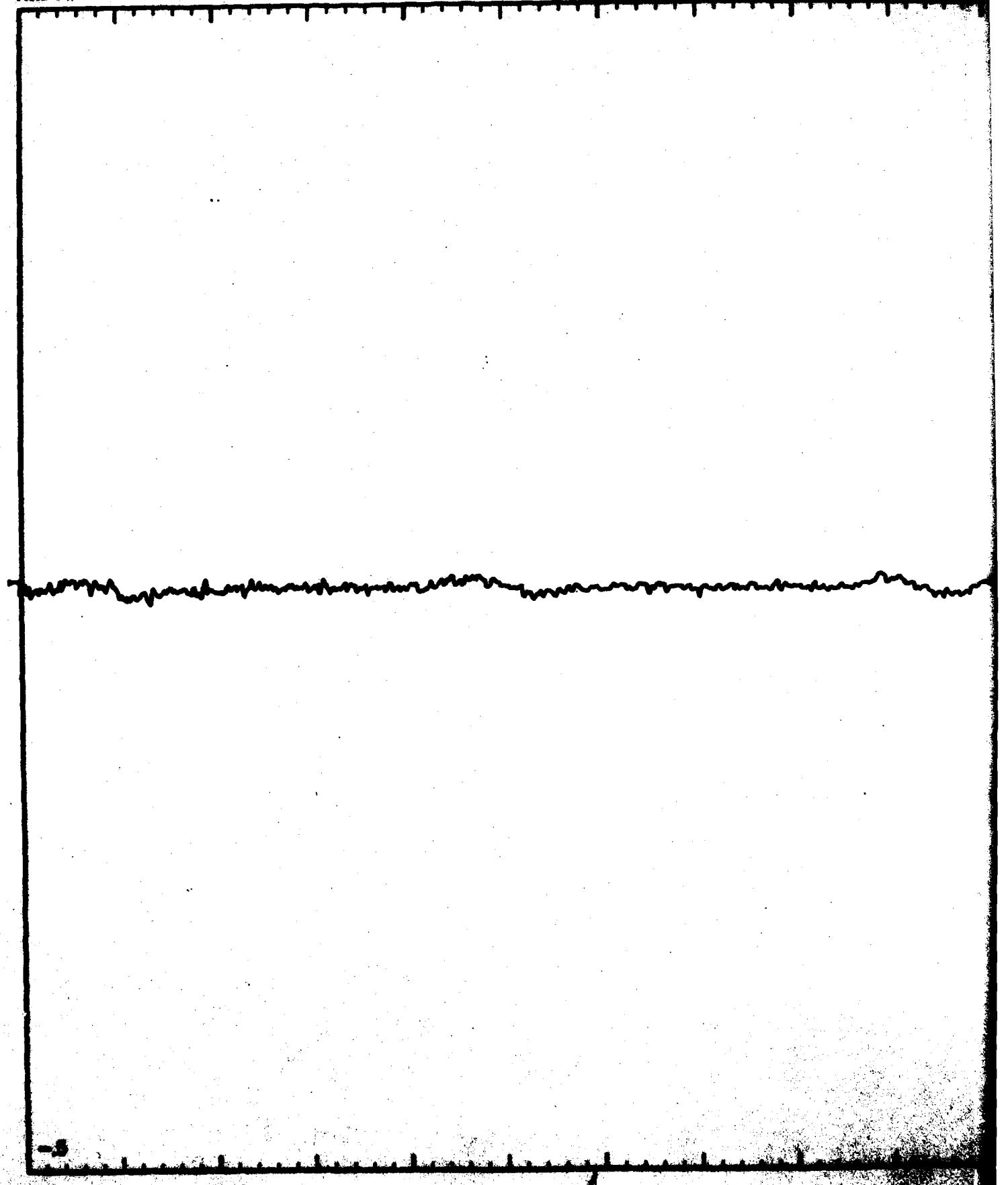

mW J Kennett Operator

GHz 1/5/82 Date 9mm Solids Remarks

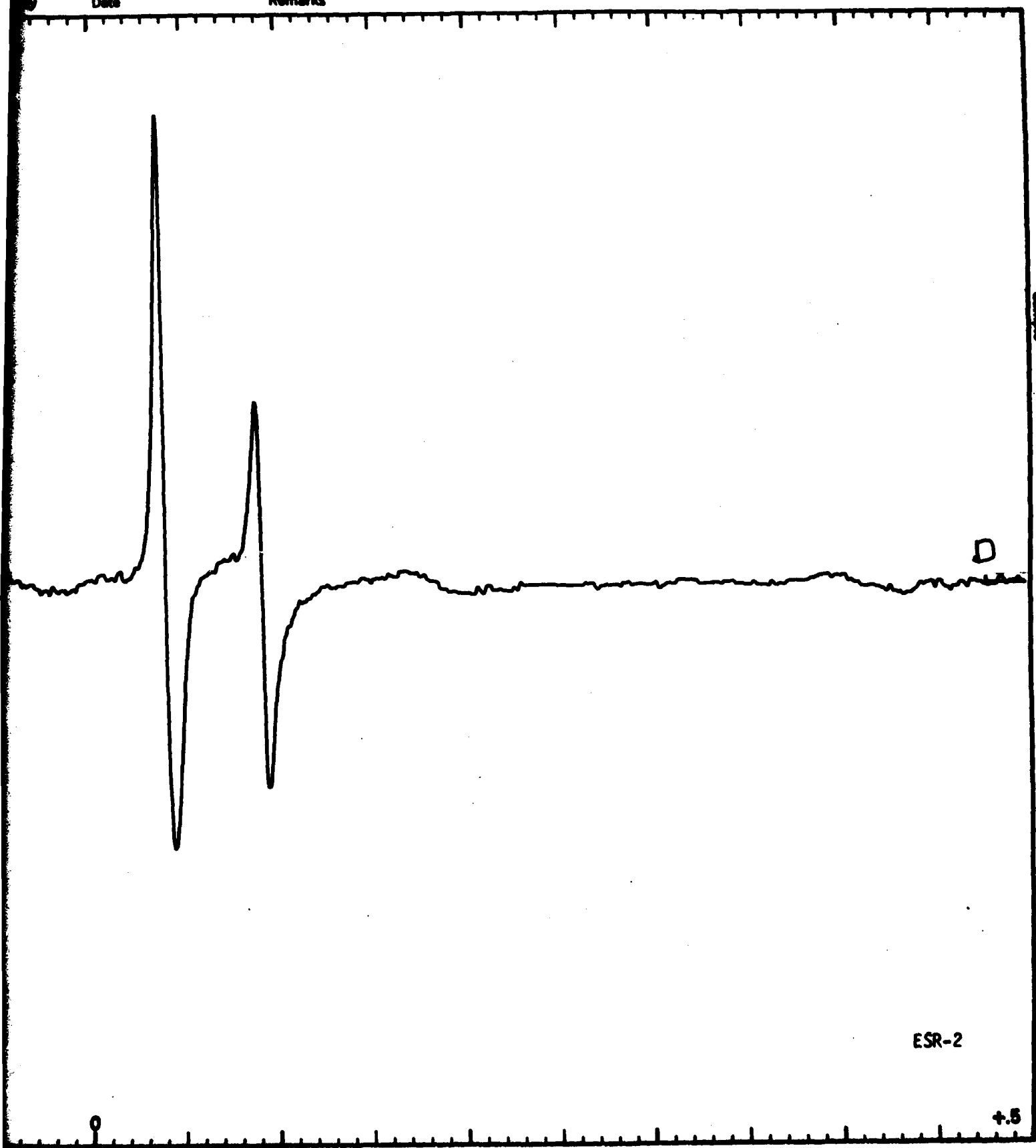

ESR CHART A

Sample 50% Overlinked 12/22/81

Spectrum No.

Scan Range	Time Constant	Modulation Amplitude	Receiver Gain	Microwave Power
4 x 100 G	1 sec	2 x 1 G	1C x 1C	1.5

Field Set	Scan Time	Modulation Frequency	Temperature	Microwave Frequency
3300 G	hrs 1C min	100 K Hz	RT °C	9.279

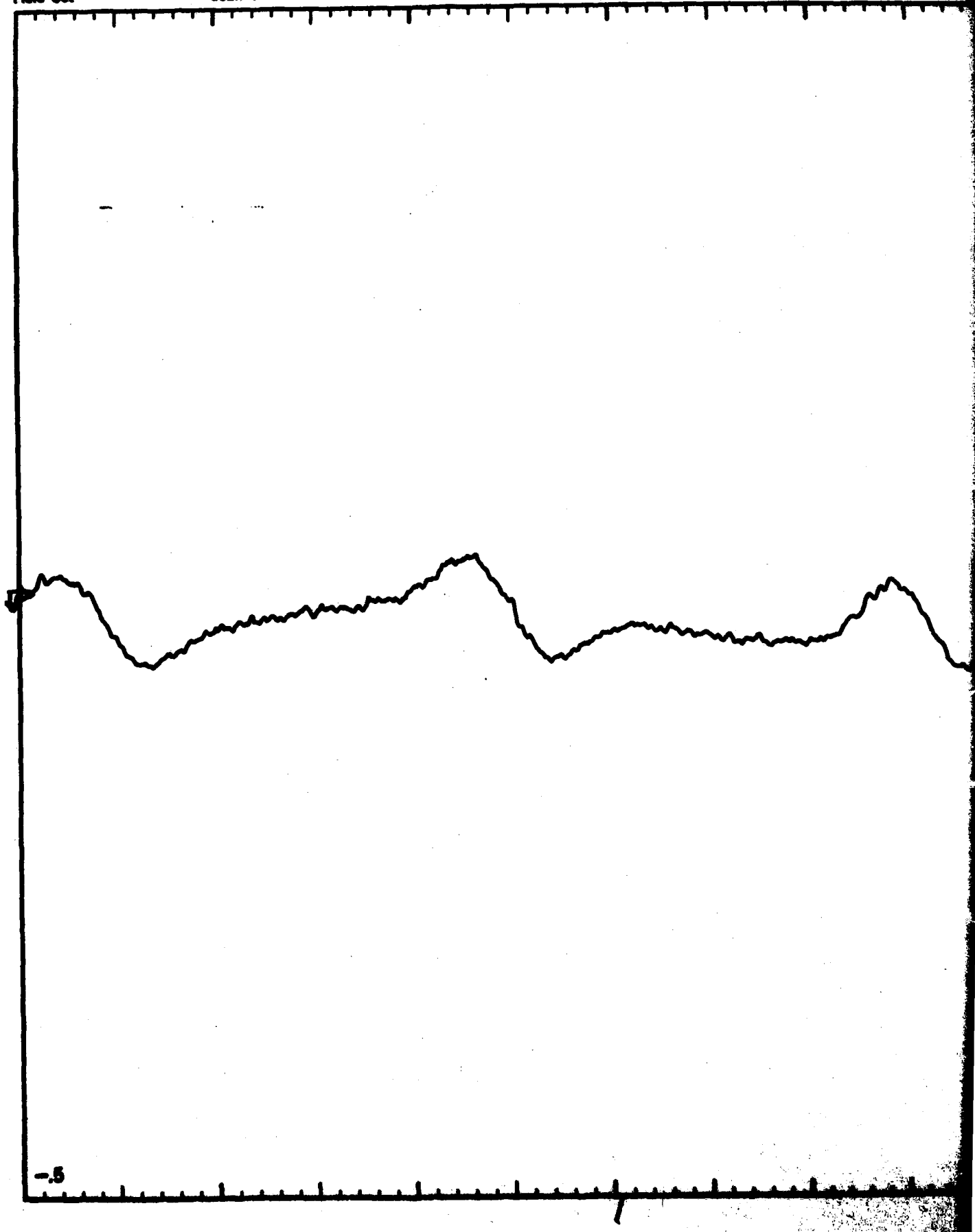

mW Operator J Kennedy

GHz Date 11/5/82 Remarks 9mm Solids

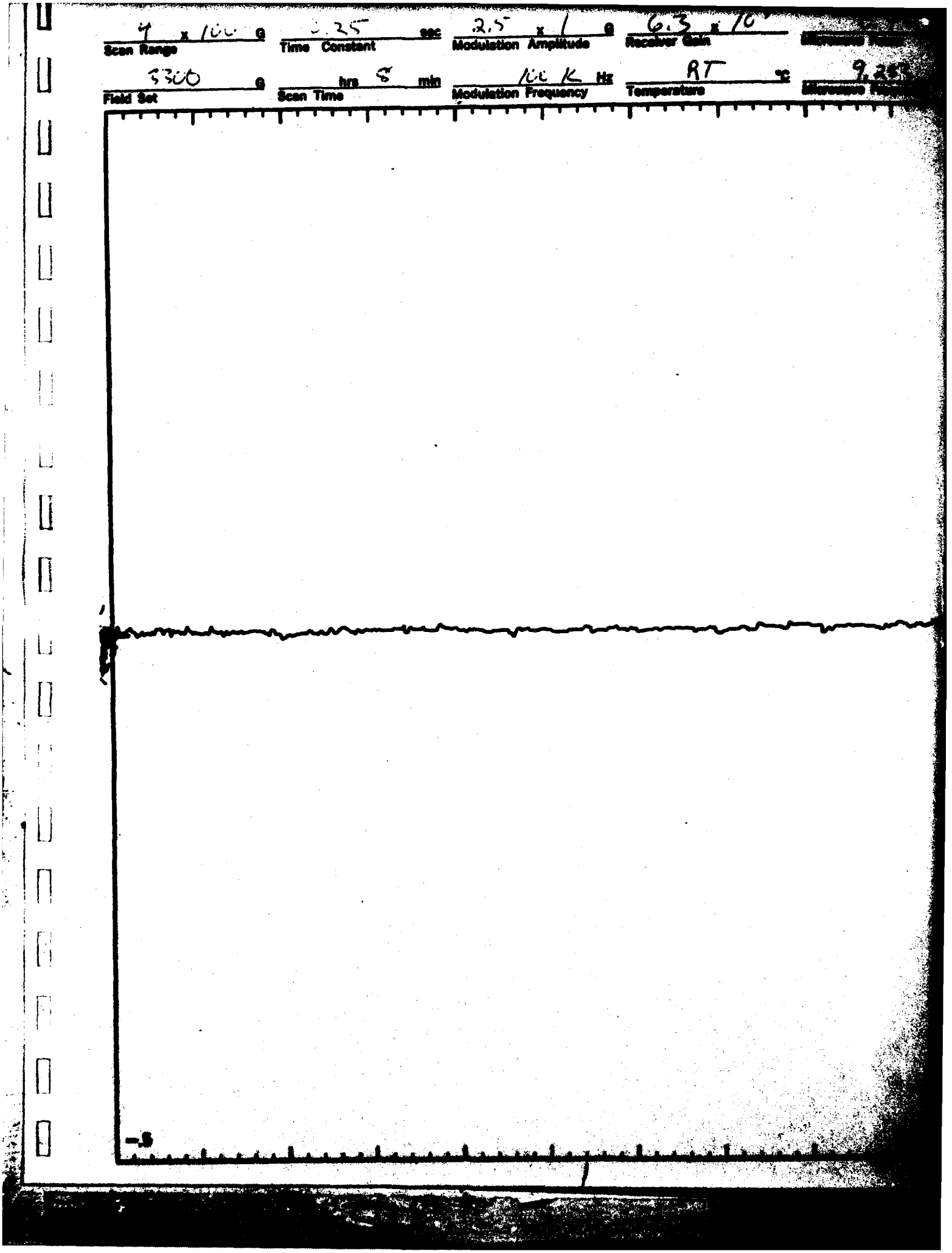
4 x 100 G
Scan Range
0.25 sec
Time Constant
2.5 x 1 G
Modulation Amplitude
6.3 x 10
Receiver Gain
3300 G
Field Set
hrs 8 min
Scan Time
100 K Hz
Modulation Frequency
RT °C
Temperature
9.25
Microwave
-5

75 mW
wer

Operator

183 GHz
equency

11/5/87
Date

O Solids
Remarks

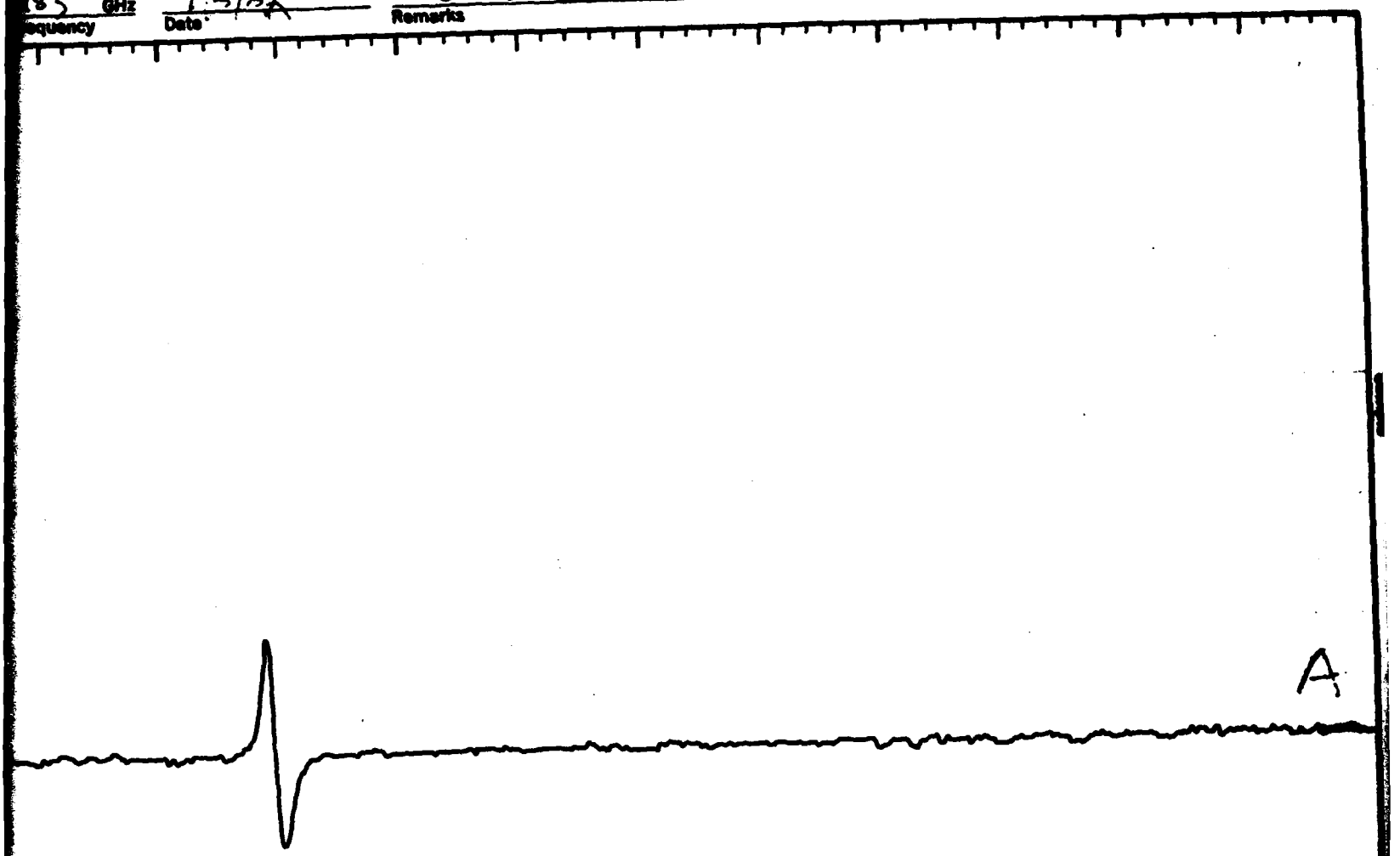

ESR-4

1

2

ELECTROLYTE FROM CELL 30% OVERDISCHARGED

% TRANSMITTANCE

-6.10 -.30 5.50 11.30 17.10 22.90 28.70 34.50 40.30 46.10

4000 3790 3580 3370 3160 2950 2740 2530 2320

2476

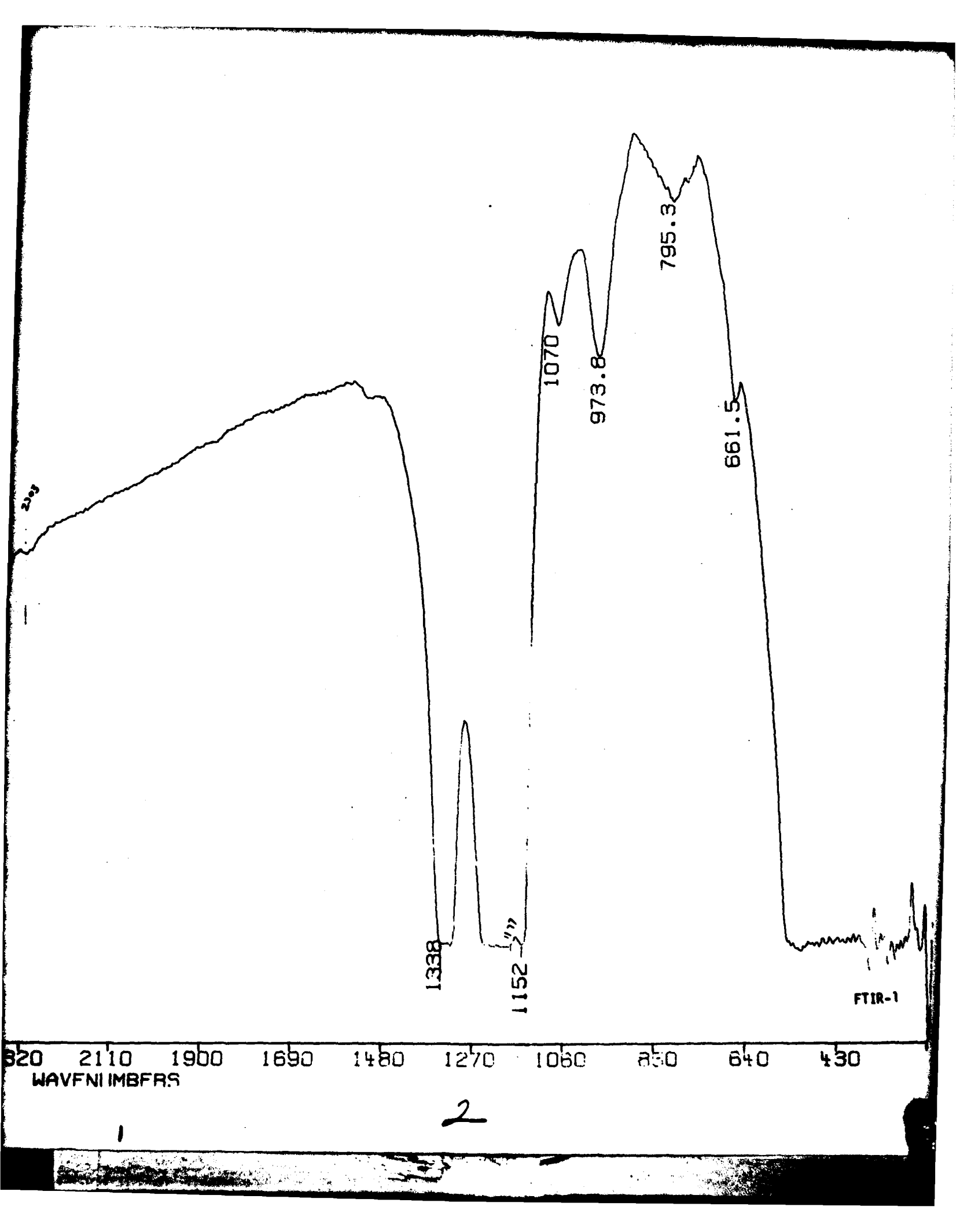
795.3
1070
973.8
661.5
1338
1152
FTIR-1
320
2110
1900
1690
1480
1270
1060
850
640
430
WAVENUMBERS

SAMPLE: ELECTROLYE FROM CELL 90% OVERDISCHARGED
2 DAYS AFTER OPENING CELL

% TRANSMITTANCE
59.40
52.70
46.00
39.30
32.60
25.90
19.20
12.50
5.80
-.90

2765
2393
2468

4000 3790 3580 3370 3160 2950 2740

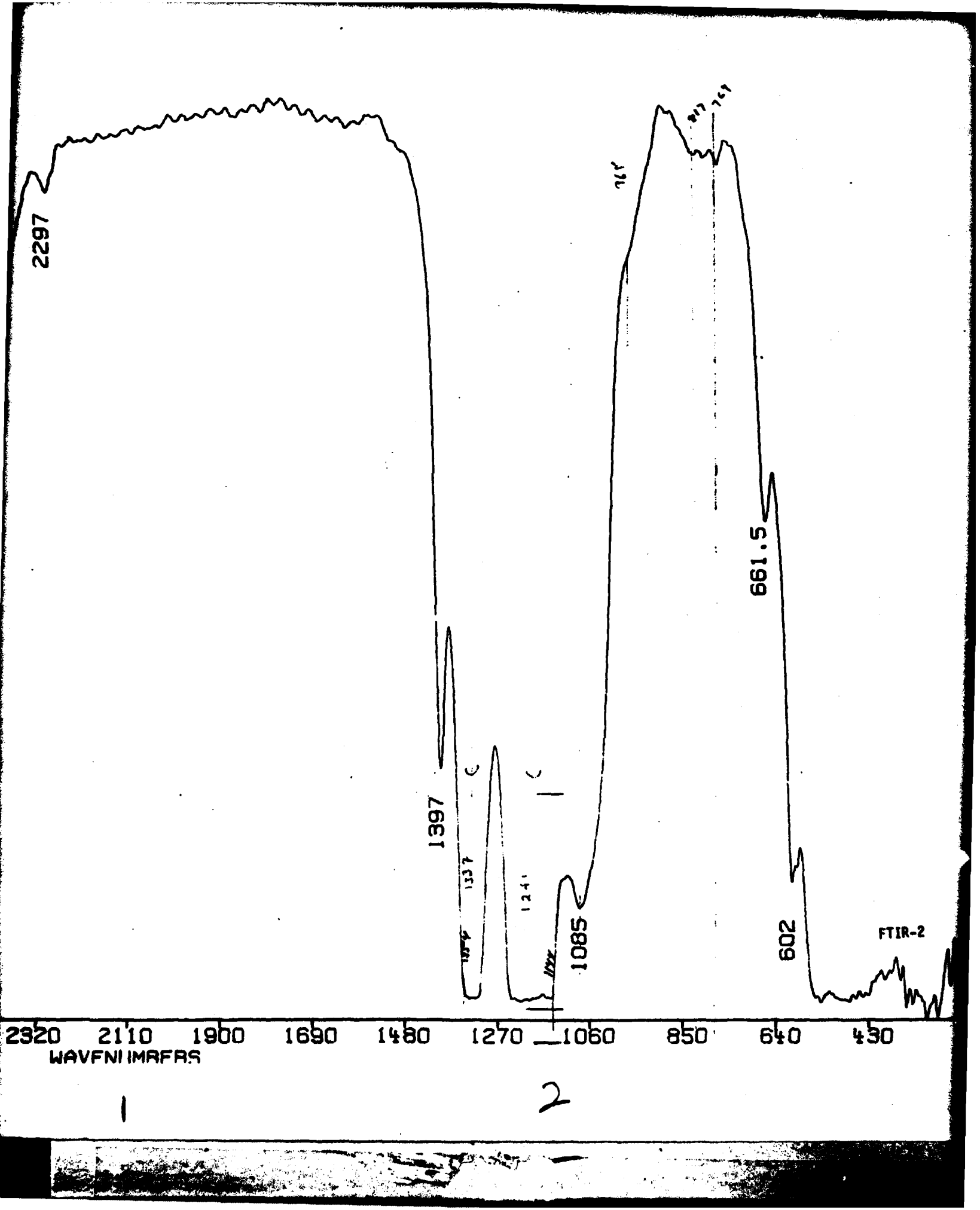
2297
1397
1337
1241
1085
767
661.5
602
FTIR-2
2320
2110
1900
1690
1480
1270
1060
850
640
430
WAVENUMBERS
1
2

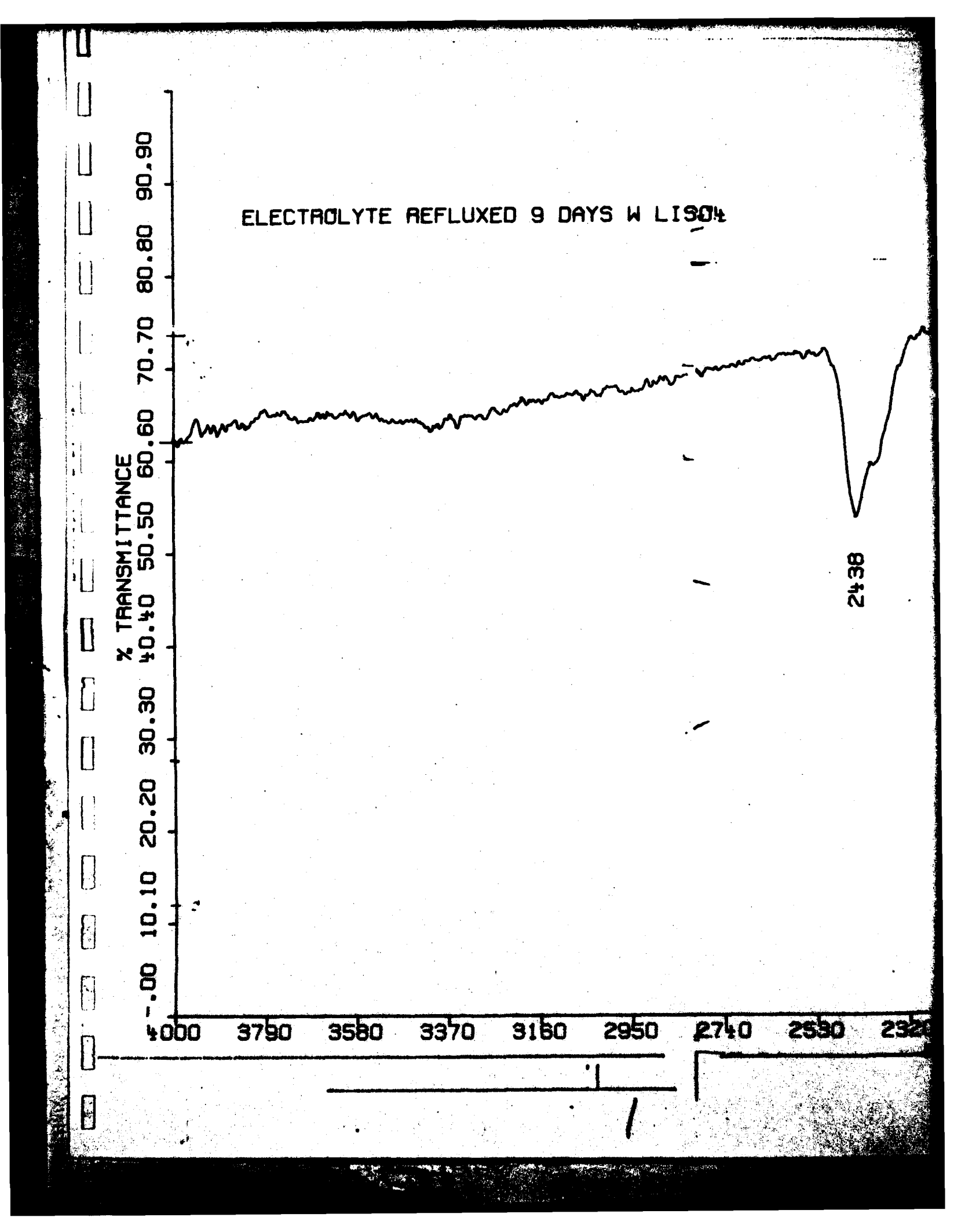
ELECTROLYTE REFLUXED 9 DAYS W LISO4
% TRANSMITTANCE
-.00
10.10
20.20
30.30
40.40
50.50
60.60
70.70
80.80
90.90
4000
3790
3580
3370
3160
2950
2740
2530
2438

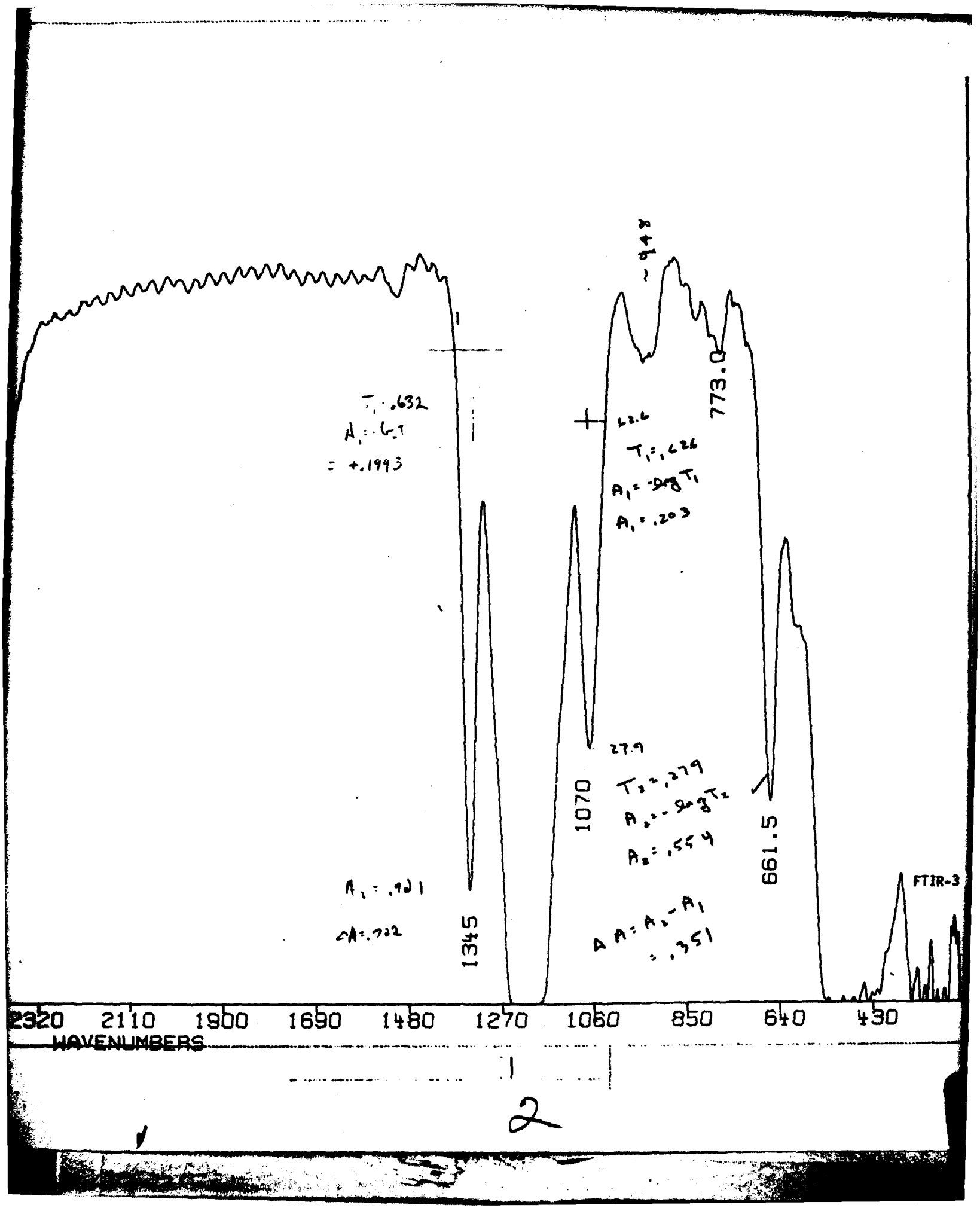
~948
773.0
T₁: .632
A₁: -log T
= +.1993
62.6
T₁: .626
A₁: -log T₁
A₁: .203
1070
27.9
T₂: .279
A₂: -log T₂
A₂: .554
661.5
A₁: .921
ΔA: .722
1345
ΔA: A₂ - A₁
: .351
FTIR-3
2320
2110
1900
1690
1480
1270
1060
850
640
430
WAVENUMBERS

2